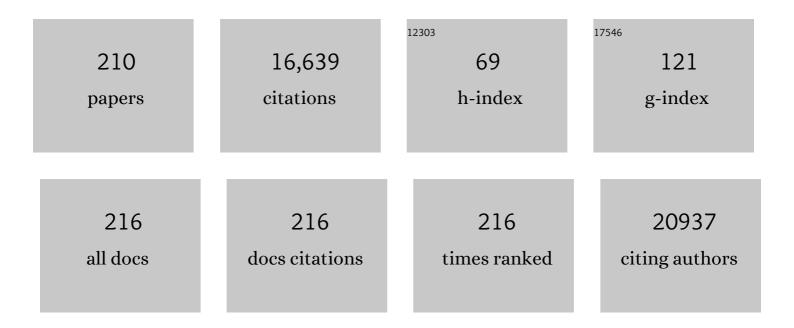
List of Publications by Year in descending order

Source: https://exaly.com/author-pdf/3429281/publications.pdf Version: 2024-02-01



SUUZUOULU

#	Article	IF	CITATIONS
1	Machine Learning: An Advanced Platform for Materials Development and State Prediction in Lithiumâ€lon Batteries. Advanced Materials, 2022, 34, e2101474.	11.1	140
2	Molecule functionalization to facilitate electrocatalytic oxygen reduction on graphdiyne. Journal of Energy Chemistry, 2022, 65, 141-148.	7.1	11
3	Metalâ€ion Oligomerization Inside Electrified Carbon Micropores and its Effect on Capacitive Charge Storage. Advanced Materials, 2022, 34, e2107439.	11.1	24
4	Mg-stabilized subnanometer Rh particles in zeolite Beta as highly efficient catalysts for selective hydrogenation. Journal of Catalysis, 2022, 405, 489-498.	3.1	8
5	Synergistic effect of Ru-N4 sites and Cu-N3 sites in carbon nitride for highly selective photocatalytic reduction of CO2 to methane. Applied Catalysis B: Environmental, 2022, 307, 121154.	10.8	57
6	Thermoelectric properties of organic charge transfer salts from first-principles investigations: role of molecular packing and triiodide anions. Journal of Materials Chemistry A, 2022, 10, 4288-4299.	5.2	1
7	Electronegativityâ€Induced Charge Balancing to Boost Stability and Activity of Amorphous Electrocatalysts. Advanced Materials, 2022, 34, e2100537.	11.1	39
8	Noble metal alloy thin films by atomic layer deposition and rapid Joule heating. Scientific Reports, 2022, 12, 2522.	1.6	12
9	Crossover between Bulk and Interface Photovoltaic Mechanisms in a Ferroelectric Vertical Heterostructure. Physical Review Applied, 2022, 17, .	1.5	6
10	Mechanical influence of graphene oxide in the interface between calcium silicate hydrate and quartz: A molecular dynamics study. Construction and Building Materials, 2022, 325, 126597.	3.2	5
11	A Defect Engineered Electrocatalyst that Promotes High-Efficiency Urea Synthesis under Ambient Conditions. ACS Nano, 2022, 16, 8213-8222.	7.3	109
12	1,3,5â€Triphenylbenzene Based Porous Conjugated Polymers for Highly Efficient Photoreduction of Lowâ€Concentration CO ₂ in the Gasâ€Phase System. Solar Rrl, 2022, 6, .	3.1	8
13	Efficient CO ₂ Electroreduction to Ethanol by Cu ₃ Sn Catalyst. Small Methods, 2022, 6, e2101334.	4.6	39
14	Dataâ€Ðriven Materials Innovation and Applications. Advanced Materials, 2022, 34, e2104113.	11.1	51
15	Holey Reduced Graphene Oxide Scaffolded Heterocyclic Aramid Fibers with Enhanced Mechanical Performance. Advanced Functional Materials, 2022, 32, .	7.8	14
16	Reversible Al Metal Anodes Enabled by Amorphization for Aqueous Aluminum Batteries. Journal of the American Chemical Society, 2022, 144, 11444-11455.	6.6	63
17	Directing the Architecture of Surface-Clean Cu ₂ O for CO Electroreduction. Journal of the American Chemical Society, 2022, 144, 12410-12420.	6.6	24
18	Cobalt nitride as a novel cocatalyst to boost photocatalytic CO2 reduction. Nano Energy, 2021, 79, 105429.	8.2	117

#	Article	IF	CITATIONS
19	Product-Specific Active Site Motifs of Cu for Electrochemical CO2 Reduction. CheM, 2021, 7, 406-420.	5.8	72
20	Understanding the Activity of Carbon-Based Single-Atom Electrocatalysts from <i>Ab Initio</i> Simulations. , 2021, 3, 110-120.		19
21	Addressing molecular optomechanical effects in nanocavity-enhanced Raman scattering beyond the single plasmonic mode. Nanoscale, 2021, 13, 1938-1954.	2.8	19
22	2,4,6â€Triphenylâ€1,3,5â€Triazine Based Covalent Organic Frameworks for Photoelectrochemical H ₂ Evolution. Advanced Materials Interfaces, 2021, 8, 2002191.	1.9	40
23	3d Transitionâ€Metalâ€Mediated Columbite Nanocatalysts for Decentralized Electrosynthesis of Hydrogen Peroxide. Small, 2021, 17, e2007249.	5.2	35
24	Fluorination-Guided Li-Anchoring Behaviors on Phthalocyanines. Journal of Physical Chemistry C, 2021, 125, 8236-8243.	1.5	3
25	In Situ and Quantitative Vapor/Solid Anion Exchange for Composition Regulation and Optical Properties of Perovskites. Advanced Optical Materials, 2021, 9, 2002186.	3.6	7
26	Enhanced Electrochemical Methanation of Carbon Dioxide at the Single-Layer Hexagonal Boron Nitride/Cu Interfacial Perimeter. Nano Letters, 2021, 21, 4469-4476.	4.5	16
27	Graphdiyne/Graphene Heterostructure: A Universal 2D Scaffold Anchoring Monodispersed Transition-Metal Phthalocyanines for Selective and Durable CO ₂ Electroreduction. Journal of the American Chemical Society, 2021, 143, 8679-8688.	6.6	87
28	Selective electrocatalytic synthesis of urea with nitrate and carbon dioxide. Nature Sustainability, 2021, 4, 868-876.	11.5	264
29	Accurate machine learning models based on small dataset of energetic materials through spatial matrix featurization methods. Journal of Energy Chemistry, 2021, 63, 364-375.	7.1	7
30	Surface Local Polarization Induced by Bismuthâ€Oxygen Vacancy Pairs Tuning Non ovalent Interaction for CO ₂ Photoreduction. Advanced Energy Materials, 2021, 11, 2102389.	10.2	109
31	Flow Direction-Dependent Elastic Instability in a Symmetry-Breaking Microchannel. Micromachines, 2021, 12, 1139.	1.4	1
32	Dynamic Restructuring of Cuâ€Đoped SnS ₂ Nanoflowers for Highly Selective Electrochemical CO ₂ Reduction to Formate. Angewandte Chemie, 2021, 133, 26437-26441.	1.6	8
33	Dynamic Restructuring of Cuâ€Đoped SnS ₂ Nanoflowers for Highly Selective Electrochemical CO ₂ Reduction to Formate. Angewandte Chemie - International Edition, 2021, 60, 26233-26237.	7.2	66
34	Lattice strain and atomic replacement of CoO6 octahedra in layered sodium cobalt oxide for boosted water oxidation electrocatalysis. Applied Catalysis B: Environmental, 2021, 297, 120477.	10.8	30
35	Boosting the water dissociation kinetics <i>via</i> charge redistribution of ruthenium decorated on S, N-codoped carbon. Journal of Materials Chemistry A, 2021, 9, 16967-16973.	5.2	19
36	Atomic layer deposition of rhodium and palladium thin film using low-concentration ozone. RSC Advances, 2021, 11, 22773-22779.	1.7	12

#	Article	IF	CITATIONS
37	First-principles study of the anisotropic thermal expansion and thermal transport properties in h-BN. Science China Materials, 2021, 64, 953-963.	3.5	14
38	Atomic layer deposition of palladium thin film from palladium (II) hexafluoroacetylacetonate and ozone reactant. Thin Solid Films, 2021, 738, 138955.	0.8	7
39	Free-standing 2D non-van der Waals antiferromagnetic hexagonal FeSe semiconductor: halide-assisted chemical synthesis and Fe ²⁺ related magnetic transitions. Chemical Science, 2021, 13, 203-209.	3.7	14
40	Adsorption and Reaction Mechanisms of Direct Palladium Synthesis by ALD Using Pd(hfac)2 and Ozone on Si (100) Surface. Processes, 2021, 9, 2246.	1.3	2
41	Deformable Thermo-Responsive Smart Windows Based on a Shape Memory Polymer for Adaptive Solar Modulations. ACS Applied Materials & Interfaces, 2021, 13, 61196-61204.	4.0	16
42	Influence of functionalized core–shell structure on the thermodynamic and shape memory properties of nanocomposites. Nanoscale, 2020, 12, 3205-3219.	2.8	6
43	Chirality Evolution from Sub-1 Nanometer Nanowires to the Macroscopic Helical Structure. Journal of the American Chemical Society, 2020, 142, 1375-1381.	6.6	47
44	Octahedral Coordinated Trivalent Cobalt Enriched Multimetal Oxygenâ€Evolution Catalysts. Advanced Energy Materials, 2020, 10, 2002593.	10.2	47
45	Strain-Engineering of Bi ₁₂ O ₁₇ Br ₂ Nanotubes for Boosting Photocatalytic CO ₂ Reduction. , 2020, 2, 1025-1032.		82
46	Modulating Orientational Order to Organize Polyhedral Nanoparticles into Plastic Crystals and Uniform Metacrystals. Angewandte Chemie - International Edition, 2020, 59, 21183-21189.	7.2	7
47	An in-situ spectroscopy investigation of alkali metal interaction mechanism with the imide functional group. Nano Research, 2020, 13, 3224-3229.	5.8	11
48	Boosting Electrocatalytic Ammonia Production through Mimicking "π Back-Donation― CheM, 2020, 6, 2690-2702.	5.8	88
49	Modulating Orientational Order to Organize Polyhedral Nanoparticles into Plastic Crystals and Uniform Metacrystals. Angewandte Chemie, 2020, 132, 21369-21375.	1.6	3
50	Oneâ€Đimensional <i>Ï€</i> –d Conjugated Coordination Polymer for Electrochromic Energy Storage Device with Exceptionally High Performance. Advanced Science, 2020, 7, 1903109.	5.6	72
51	Alkali metal storage mechanism in organic semiconductor of perylene-3,4,9,10-tetracarboxylicdianhydride. Applied Surface Science, 2020, 524, 146396.	3.1	13
52	Covalency competition dominates the water oxidation structure–activity relationship on spinel oxides. Nature Catalysis, 2020, 3, 554-563.	16.1	284
53	Smart Windows: 3D Printed Smart Windows for Adaptive Solar Modulations (Advanced Optical) Tj ETQq1 1 0.78	34314 rgB ⁻ 3.6	T /Qverlock
54	<i>In situ</i> growth of Au–Ag bimetallic nanorings on optical fibers for enhanced plasmonic serving lowrnal of Materials Chemistry C. 2020. 8, 7552,7560.	2.7	8

sensing. Journal of Materials Chemistry C, 2020, 8, 7552-7560.

#	Article	IF	CITATIONS
55	Unconventional Oxygen Reduction Reaction Mechanism and Scaling Relation on Single-Atom Catalysts. ACS Catalysis, 2020, 10, 4313-4318.	5.5	119
56	3D Printed Smart Windows for Adaptive Solar Modulations. Advanced Optical Materials, 2020, 8, 200013.	3.6	28
57	Hierarchically porous Cu/Zn bimetallic catalysts for highly selective CO2 electroreduction to liquid C2 products. Applied Catalysis B: Environmental, 2020, 269, 118800.	10.8	108
58	Improving the accuracy of converting dose to medium to dose to water algorithms in small megavoltage photon fields in dose to medium based treatment planning systems. Physica Medica, 2020, 71, 62-70.	0.4	2
59	Thermalâ€Disrupting Interface Mitigates Intercellular Cohesion Loss for Accurate Topical Antibacterial Therapy. Advanced Materials, 2020, 32, e1907030.	11.1	75
60	van der Waals Heterojunction between a Bottom-Up Grown Doped Graphene Quantum Dot and Graphene for Photoelectrochemical Water Splitting. ACS Nano, 2020, 14, 1185-1195.	7.3	100
61	Broadband high-performance electromagnetic wave absorption of Co-doped NiZn ferrite/polyaniline on MXenes. Ceramics International, 2020, 46, 10006-10015.	2.3	64
62	Structures and Antifouling Properties of Self-Assembled Zwitterionic Peptide Monolayers: Effects of Peptide Charge Distributions and Divalent Cations. Biomacromolecules, 2020, 21, 2087-2095.	2.6	32
63	Multiscale Structure Construction by Layer-by-Layer Self-Assembly to Modify the Carbon Fiber Surface. Journal of Physical Chemistry C, 2020, 124, 10733-10743.	1.5	6
64	Oxygen vacancy mediated bismuth stannate ultra-small nanoparticle towards photocatalytic CO2-to-CO conversion. Applied Catalysis B: Environmental, 2020, 276, 119156.	10.8	59
65	Strong dependence of the vertical charge carrier mobility on the ï€â€"ï€ stacking distance in molecule/graphene heterojunctions. Physical Chemistry Chemical Physics, 2020, 22, 13802-13807.	1.3	10
66	Broadband Extrinsic Selfâ€Trapped Exciton Emission in Snâ€Doped 2D Leadâ€Halide Perovskites. Advanced Materials, 2019, 31, e1806385.	11.1	198
67	Atomic Pd on Graphdiyne/Graphene Heterostructure as Efficient Catalyst for Aromatic Nitroreduction. Advanced Functional Materials, 2019, 29, 1905423.	7.8	112
68	Incorporation of clusters within inorganic materials through their addition during nucleation steps. Nature Chemistry, 2019, 11, 839-845.	6.6	104
69	Self curing and voltage activated catechol adhesives. Chemical Communications, 2019, 55, 10076-10079.	2.2	19
70	Crystal phase effect upon O ₂ activation on gold surfaces through intrinsic strain. Nanoscale, 2019, 11, 14587-14591.	2.8	3
71	Optically Governed Dynamic Surface Charge Redistribution of Hybrid Plasmoâ€₽yroelectric Nanosystems. Small, 2019, 15, e1903042.	5.2	12
72	Bismuth Vacancy-Tuned Bismuth Oxybromide Ultrathin Nanosheets toward Photocatalytic CO ₂ Reduction. ACS Applied Materials & Interfaces, 2019, 11, 30786-30792.	4.0	140

#	Article	IF	CITATIONS
73	Facile and versatile access to substituted hexabenzoovalene derivatives: characterization and optoelectronic properties. Organic and Biomolecular Chemistry, 2019, 17, 7964-7972.	1.5	6
74	Isolated single atom cobalt in Bi3O4Br atomic layers to trigger efficient CO2 photoreduction. Nature Communications, 2019, 10, 2840.	5.8	327
75	Interfacing Epitaxial Dinickel Phosphide to 2D Nickel Thiophosphate Nanosheets for Boosting Electrocatalytic Water Splitting. ACS Nano, 2019, 13, 7975-7984.	7.3	171
76	Tunable Subradiant Mode in Free-Standing Metallic Nanohole Arrays for High-Performance Plasmofluidic Sensing. Journal of Physical Chemistry C, 2019, 123, 25394-25401.	1.5	12
77	Synergy of Dopants and Defects in Graphitic Carbon Nitride with Exceptionally Modulated Band Structures for Efficient Photocatalytic Oxygen Evolution. Advanced Materials, 2019, 31, e1903545.	11.1	604
78	Interfacial Latticeâ€Strainâ€Driven Generation of Oxygen Vacancies in an Aerobicâ€Annealed TiO ₂ (B) Electrode. Advanced Materials, 2019, 31, e1906156.	11.1	53
79	Ru@UiO-66(Ce) catalyzed acceptorless dehydrogenation of primary amines to nitriles: the roles of Lewis acid–base pairs in the reaction. Green Chemistry, 2019, 21, 5386-5393.	4.6	37
80	Development of trans-1,4-polyisoprene (TPI) nanocomposite reinforced with nano-SiO2 functionalized graphene oxide. Colloids and Surfaces A: Physicochemical and Engineering Aspects, 2019, 580, 123790.	2.3	9
81	Development of functionalized core–shell nanohybrid/synthetic rubber nanocomposites with enhanced performance. Soft Matter, 2019, 15, 8338-8351.	1.2	6
82	Impact of Stoichiometry and Fluorine Atoms on the Charge Transport of Perylene–F ₄ TCNQ. Journal of Physical Chemistry Letters, 2019, 10, 3376-3380.	2.1	15
83	Stereodefined Codoping of sp-N and S Atoms in Few-Layer Graphdiyne for Oxygen Evolution Reaction. Journal of the American Chemical Society, 2019, 141, 7240-7244.	6.6	198
84	An Allâ€Inorganic Colloidal Nanocrystal Flexible Polarizer. Angewandte Chemie - International Edition, 2019, 58, 8730-8735.	7.2	39
85	Vacancy-Driven Stabilization of the Cubic Perovskite Polymorph of CsPbI ₃ . Journal of Physical Chemistry C, 2019, 123, 9735-9744.	1.5	47
86	Continuous rapid dechlorination of p-chlorophenol by Fe-Pd nanoparticles promoted by procyanidin. Chemical Engineering Science, 2019, 201, 121-131.	1.9	15
87	First-Principles Study on Structural, Electronic, and Optical Properties of Inorganic Ge-Based Halide Perovskites. Inorganic Chemistry, 2019, 58, 4134-4140.	1.9	68
88	Triphenylamine based conjugated microporous polymers for selective photoreduction of CO ₂ to CO under visible light. Green Chemistry, 2019, 21, 6606-6610.	4.6	58
89	Electrode Materials: Interfacial Latticeâ€Strainâ€Driven Generation of Oxygen Vacancies in an Aerobicâ€Annealed TiO ₂ (B) Electrode (Adv. Mater. 52/2019). Advanced Materials, 2019, 31, 1970367.	11.1	9
90	Electrical promotion of spatially photoinduced charge separation via interfacial-built-in quasi-alloying effect in hierarchical Zn2In2S5/Ti3C2(O, OH)x hybrids toward efficient photocatalytic hydrogen evolution and environmental remediation. Applied Catalysis B: Environmental, 2019, 245, 290-301.	10.8	229

#	Article	IF	CITATIONS
91	Achieving highly efficient electrocatalytic oxygen evolution with ultrathin 2D Fe-doped nickel thiophosphate nanosheets. Nano Energy, 2018, 47, 257-265.	8.2	122
92	Oxocarbon-functionalized graphene as a lithium-ion battery cathode: a first-principles investigation. Physical Chemistry Chemical Physics, 2018, 20, 7447-7456.	1.3	15
93	Photogenerated charge transfer via interfacial internal electric field for significantly improved photocatalysis in direct Z-scheme oxygen-doped carbon nitrogen/CoAl-layered double hydroxide heterojunction. Applied Catalysis B: Environmental, 2018, 227, 530-540.	10.8	219
94	Quantitative investigation on the critical thickness of the dielectric shell for metallic nanoparticles determined by the plasmon decay length. Nanotechnology, 2018, 29, 165501.	1.3	3
95	Quantitative Prediction of Position and Orientation for Platonic Nanoparticles at Liquid/Liquid Interfaces. Journal of Physical Chemistry Letters, 2018, 9, 373-382.	2.1	15
96	Site‣elective Catalysis of a Multifunctional Linear Molecule: The Steric Hindrance of Metal–Organic Framework Channels. Advanced Materials, 2018, 30, e1800643.	11.1	62
97	Realizing a Record Photothermal Conversion Efficiency of Spiky Gold Nanoparticles in the Second Near-Infrared Window by Structure-Based Rational Design. Chemistry of Materials, 2018, 30, 2709-2718.	3.2	85
98	Crystal phase-based epitaxial growth of hybrid noble metal nanostructures on 4H/fcc Au nanowires. Nature Chemistry, 2018, 10, 456-461.	6.6	220
99	Rattle-type Au@Cu 2â ^{~*} x S hollow mesoporous nanocrystals with enhanced photothermal efficiency for intracellular oncogenic microRNA detection and chemo-photothermal therapy. Biomaterials, 2018, 158, 23-33.	5.7	68
100	Direct Experimental Observation of Facetâ€Đependent SERS of Cu ₂ O Polyhedra. Small, 2018, 14, 1703274.	5.2	108
101	Spatially Probed Plasmonic Photothermic Nanoheater Enhanced Hybrid Polymeric–Metallic PVDFâ€Ag Nanogenerator. Small, 2018, 14, 1702268.	5.2	23
102	Solution Adsorption Formation of a π onjugated Polymer/Graphene Composite for Highâ€Performance Fieldâ€Effect Transistors. Advanced Materials, 2018, 30, 1705377.	11.1	48
103	Ultranarrow Graphene Nanoribbons toward Oxygen Reduction and Evolution Reactions. Advanced Science, 2018, 5, 1801375.	5.6	59
104	Donor–Acceptor Fluorophores for Energy-Transfer-Mediated Photocatalysis. Journal of the American Chemical Society, 2018, 140, 13719-13725.	6.6	174
105	Yin-Yang Harmony: Metal and Nonmetal Dual-Doping Boosts Electrocatalytic Activity for Alkaline Hydrogen Evolution. ACS Energy Letters, 2018, 3, 2750-2756.	8.8	154
106	Mosaicâ€Structured Cobalt Nickel Thiophosphate Nanosheets Incorporated Nâ€doped Carbon for Efficient and Stable Electrocatalytic Water Splitting. Advanced Functional Materials, 2018, 28, 1805075.	7.8	57
107	Highly-sensitive optical organic vapor sensor through polymeric swelling induced variation of fluorescent intensity. Nature Communications, 2018, 9, 3799.	5.8	86
108	Mechano-regulated metal–organic framework nanofilm for ultrasensitive and anti-jamming strain sensing. Nature Communications, 2018, 9, 3813.	5.8	57

#	Article	IF	CITATIONS
109	Exploring Peltier effect in organic thermoelectric films. Nature Communications, 2018, 9, 3586.	5.8	65
110	An electron deficiency strategy for enhancing hydrogen evolution on CoP nano-electrocatalysts. Nano Energy, 2018, 50, 273-280.	8.2	89
111	Bismuth vacancy mediated single unit cell Bi2WO6 nanosheets for boosting photocatalytic oxygen evolution. Applied Catalysis B: Environmental, 2018, 238, 119-125.	10.8	173
112	Selective hydrogenation of phenol to cyclohexanone by SiO2-supported rhodium nanoparticles under mild conditions. Journal of Catalysis, 2018, 364, 354-365.	3.1	57
113	Target-Triggered Catalytic Hairpin Assembly-Induced Core–Satellite Nanostructures for High-Sensitive "Off-to-On―SERS Detection of Intracellular MicroRNA. Analytical Chemistry, 2018, 90, 10591-10599.	3.2	85
114	Defect and pyridinic nitrogen engineering of carbon-based metal-free nanomaterial toward oxygen reduction. Nano Energy, 2018, 52, 307-314.	8.2	176
115	Creating two self-assembly micro-environments to achieve supercrystals with dual structures using polyhedral nanoparticles. Nature Communications, 2018, 9, 2769.	5.8	46
116	Performance-improved Li-O ₂ batteries by tailoring the phases of Mo _x C porous nanorods as an efficient cathode. Nanoscale, 2018, 10, 14877-14884.	2.8	28
117	Valence Electron Density-Dependent Pseudopermittivity for Nonlocal Effects in Optical Properties of Metallic Nanoparticles. ACS Photonics, 2018, 5, 2295-2304.	3.2	12
118	Morphological effects on the selectivity of intramolecular versus intermolecular catalytic reaction on Au nanoparticles. Nanoscale, 2017, 9, 7727-7733.	2.8	17
119	Gold mesoflowers with a high density of multilevel long sharp tips: synthesis and characterization. Journal of Materials Chemistry C, 2017, 5, 4884-4891.	2.7	11
120	Highly efficient and durable MoNiNC catalyst for hydrogen evolution reaction. Nano Energy, 2017, 37, 1-6.	8.2	79
121	Synthesis, Full Characterization, and Field Effect Transistor Behavior of a Stable Pyrene-Fused <i>N</i> -Heteroacene with Twelve Linearly Annulated Six-Membered Rings. Chemistry of Materials, 2017, 29, 4172-4175.	3.2	131
122	Al ₂ O ₃ Surface Complexation for Photocatalytic Organic Transformations. Journal of the American Chemical Society, 2017, 139, 269-276.	6.6	64
123	Revealing Cation-Exchange-Induced Phase Transformations in Multielemental Chalcogenide Nanoparticles. Chemistry of Materials, 2017, 29, 9192-9199.	3.2	19
124	Monodisperse Dual Plasmonic Au@Cu _{2–<i>x</i>} E (E= S, Se) Core@Shell Supraparticles: Aqueous Fabrication, Multimodal Imaging, and Tumor Therapy at <i>in Vivo</i> Level. ACS Nano, 2017, 11, 8273-8281.	7.3	139
125	Widening the Spectral Range of Ultrahigh Field Enhancement by Efficient Coupling of Localized to Extended Plasmons and Cavity Resonances in Grating Geometry. Journal of Physical Chemistry C, 2017, 121, 27612-27623.	1.5	22
126	Remarkable SERS Activity Observed from Amorphous ZnO Nanocages. Angewandte Chemie - International Edition, 2017, 56, 9851-9855.	7.2	238

#	Article	IF	CITATIONS
127	Defect engineering in atomically-thin bismuth oxychloride towards photocatalytic oxygen evolution. Journal of Materials Chemistry A, 2017, 5, 14144-14151.	5.2	107
128	Remarkable SERS Activity Observed from Amorphous ZnO Nanocages. Angewandte Chemie, 2017, 129, 9983-9987.	1.6	47
129	Quantitative prediction of the position and orientation for an octahedral nanoparticle at liquid/liquid interfaces. Nanoscale, 2017, 9, 11239-11248.	2.8	11
130	Poor Photovoltaic Performance of Cs ₃ Bi ₂ I ₉ : An Insight through First-Principles Calculations. Journal of Physical Chemistry C, 2017, 121, 17062-17067.	1.5	121
131	Dually Ordered Porous TiO ₂ â€rGO Composites with Controllable Light Absorption Properties for Efficient Solar Energy Conversion. Advanced Materials, 2017, 29, 1604795.	11.1	66
132	Alcoholâ€Mediated Resistanceâ€Switching Behavior in Metal–Organic Frameworkâ€Based Electronic Devices. Angewandte Chemie, 2016, 128, 9030-9034.	1.6	19
133	Polymer Nanowires: Enhanced Photoresponse of Conductive Polymer Nanowires Embedded with Au Nanoparticles (Adv. Mater. 15/2016). Advanced Materials, 2016, 28, 3031-3031.	11.1	1
134	Alcoholâ€Mediated Resistanceâ€Switching Behavior in Metal–Organic Frameworkâ€Based Electronic Devices. Angewandte Chemie - International Edition, 2016, 55, 8884-8888.	7.2	72
135	Synergistic Effects of Water and Oxygen Molecule Co-adsorption on (001) Surfaces of Tetragonal CH ₃ NH ₃ Pbl ₃ : A First-Principles Study. Journal of Physical Chemistry C, 2016, 120, 28448-28455.	1.5	47
136	Optimal Interparticle Gap for Ultrahigh Field Enhancement by LSP Excitation via ESPs and Confirmation Using SERS. Journal of Physical Chemistry C, 2016, 120, 28735-28742.	1.5	28
137	Hyperlensing at NIR frequencies using a hemispherical metallic nanowire lens in a sea-urchin geometry. Nanoscale, 2016, 8, 10669-10676.	2.8	8
138	Identifying Enclosed Chemical Reaction and Dynamics at the Molecular Level Using Shell-Isolated Miniaturized Plasmonic Liquid Marble. Journal of Physical Chemistry Letters, 2016, 7, 1501-1506.	2.1	30
139	Rb as an Alternative Cation for Templating Inorganic Lead-Free Perovskites for Solution Processed Photovoltaics. Chemistry of Materials, 2016, 28, 7496-7504.	3.2	249
140	Engineering the hot spots in squared arrays of gold nanoparticles on a silver film. Nanoscale, 2016, 8, 15658-15664.	2.8	17
141	Activation Effect of Electrochemical Cycling on Gold Nanoparticles towards the Hydrogen Evolution Reaction in Sulfuric Acid. Electrochimica Acta, 2016, 209, 440-447.	2.6	32
142	Empirical structural design of core@shell Au@Ag nanoparticles for SERS applications. Journal of Materials Chemistry C, 2016, 4, 6649-6656.	2.7	27
143	Enhanced Photoresponse of Conductive Polymer Nanowires Embedded with Au Nanoparticles. Advanced Materials, 2016, 28, 2978-2982.	11.1	45
144	Highly Sensitive Electroâ€Plasmonic Switches Based on Fivefold Stellate Polyhedral Gold Nanoparticles. Small, 2015, 11, 5395-5401.	5.2	14

#	Article	IF	CITATIONS
145	Engineering Interfacial Photoâ€Induced Charge Transfer Based on Nanobamboo Array Architecture for Efficient Solarâ€toâ€Chemical Energy Conversion. Advanced Materials, 2015, 27, 2207-2214.	11.1	172
146	Ultrahigh Enhancement of Electromagnetic Fields by Exciting Localized with Extended Surface Plasmons. Journal of Physical Chemistry C, 2015, 119, 19382-19389.	1.5	59
147	Tertiary amine mediated aerobic oxidation of sulfides into sulfoxides by visible-light photoredox catalysis on TiO ₂ . Chemical Science, 2015, 6, 5000-5005.	3.7	89
148	Nanoscale surface chemistry directs the tunable assembly of silver octahedra into three two-dimensional plasmonic superlattices. Nature Communications, 2015, 6, 6990.	5.8	137
149	Surface modification-induced phase transformation of hexagonal close-packed gold square sheets. Nature Communications, 2015, 6, 6571.	5.8	195
150	Size and site dependent biological hazard potential of particulate matters collected from different heights at the vicinity of a building construction. Toxicology Letters, 2015, 238, 20-29.	0.4	18
151	Lead-free germanium iodide perovskite materials for photovoltaic applications. Journal of Materials Chemistry A, 2015, 3, 23829-23832.	5.2	841
152	Engineering Structural Diversity in Gold Nanocrystals by Ligand-Mediated Interface Control. Chemistry of Materials, 2015, 27, 8032-8040.	3.2	17
153	Plasmon-Modulated Photoluminescence of Single Gold Nanobeams. ACS Photonics, 2015, 2, 1348-1354.	3.2	15
154	Gramâ€Positive Antimicrobial Activity of Amino Acidâ€Based Hydrogels. Advanced Materials, 2015, 27, 648-654.	11.1	188
155	Refractive index dependent real-time plasmonic nanoprobes on a single silver nanocube for ultrasensitive detection of the lung cancer-associated miRNAs. Chemical Communications, 2015, 51, 294-297.	2.2	35
156	Engineering plasmonic nanorod arrays for colon cancer marker detection. Biosensors and Bioelectronics, 2015, 63, 472-477.	5.3	29
157	Dependence of Plasmonic Properties on Electron Densities for Various Coupled Au Nanostructures. Journal of Physical Chemistry C, 2014, 118, 27531-27538.	1.5	21
158	Direct evidence of plasmon enhancement on photocatalytic hydrogen generation over Au/Pt-decorated TiO ₂ nanofibers. Nanoscale, 2014, 6, 5217-5222.	2.8	143
159	Surface Plasmon Resonance Enhanced Light Absorption and Photothermal Therapy in the Second Near-Infrared Window. Journal of the American Chemical Society, 2014, 136, 15684-15693.	6.6	575
160	Large-volume hot spots in gold spiky nanoparticle dimers for high-performance surface-enhanced spectroscopy. Nanoscale, 2014, 6, 12921-12928.	2.8	42
161	Orthogonally Engineering Matrix Topography and Rigidity to Regulate Multicellular Morphology. Advanced Materials, 2014, 26, 5786-5793.	11.1	47
162	Tailoring Alphabetical Metamaterials in Optical Frequency: Plasmonic Coupling, Dispersion, and Sensing. ACS Nano, 2014, 8, 3796-3806.	7.3	42

#	Article	IF	CITATIONS
163	Synergistic Modulation of Surface Interaction to Assemble Metal Nanoparticles into Twoâ€Dimensional Arrays with Tunable Plasmonic Properties. Small, 2014, 10, 609-616.	5.2	51
164	Intelligent and Ultrasensitive Analysis of Mercury Trace Contaminants via Plasmonic Metamaterialâ€Based Surfaceâ€Enhanced Raman Spectroscopy. Small, 2014, 10, 3252-3256.	5.2	20
165	Programmable Photoâ€Electrochemical Hydrogen Evolution Based on Multiâ€Segmented CdSâ€Au Nanorod Arrays. Advanced Materials, 2014, 26, 3506-3512.	11.1	150
166	Synthesis of Spiky Ag–Au Octahedral Nanoparticles and Their Tunable Optical Properties. Journal of Physical Chemistry C, 2013, 117, 16640-16649.	1.5	44
167	Metamaterials-Based Label-Free Nanosensor for Conformation and Affinity Biosensing. ACS Nano, 2013, 7, 7583-7591.	7.3	104
168	Optimizing Electromagnetic Hotspots in Plasmonic Bowtie Nanoantennae. Journal of Physical Chemistry Letters, 2013, 4, 496-501.	2.1	138
169	Hollow Nanostructures: Efficient Ag@AgCl Cubic Cage Photocatalysts Profit from Ultrafast Plasmon-Induced Electron Transfer Processes (Adv. Funct. Mater. 23/2013). Advanced Functional Materials, 2013, 23, 2902-2902.	7.8	1
170	Efficient Ag@AgCl Cubic Cage Photocatalysts Profit from Ultrafast Plasmonâ€Induced Electron Transfer Processes. Advanced Functional Materials, 2013, 23, 2932-2940.	7.8	270
171	Synthesis of Fivefold Stellate Polyhedral Gold Nanoparticles with {110}â€Facets via a Seedâ€Mediated Growth Method. Small, 2013, 9, 705-710.	5.2	43
172	Approaching a stable, green twisted heteroacene through "clean reaction―strategy. Chemical Communications, 2012, 48, 5974.	2.2	110
173	Investigating the Effects of Solid Surfaces on Ice Nucleation. Langmuir, 2012, 28, 10749-10754.	1.6	139
174	Modeling the Effect of Small Gaps in Surface-Enhanced Raman Spectroscopy. Journal of Physical Chemistry C, 2012, 116, 1627-1637.	1.5	179
175	Structural Effects in the Electromagnetic Enhancement Mechanism of Surface-Enhanced Raman Scattering: Dipole Reradiation and Rectangular Symmetry Effects for Nanoparticle Arrays. Journal of Physical Chemistry C, 2012, 116, 17318-17327.	1.5	26
176	Unconventional Nucleation and Oriented Growth of ZIFâ€8 Crystals on Nonâ€Polar Surface. Advanced Materials, 2012, 24, 5954-5958.	11.1	46
177	Nanoparticles and theory. , 2012, , .		1
178	Elevated Ag nanohole arrays for high performance plasmonic sensors based on extraordinary optical transmission. Journal of Materials Chemistry, 2012, 22, 8903.	6.7	73
179	Free-standing one-dimensional plasmonic nanostructures. Nanoscale, 2012, 4, 66-75.	2.8	46
180	Engineering "Hot―Nanoparticles for Surfaceâ€Enhanced Raman Scattering by Embedding Reporter Molecules in Metal Layers. Small, 2012, 8, 246-251.	5.2	128

#	Article	IF	CITATIONS
181	Surface-Enhanced Raman Scattering of Ag–Au Nanodisk Heterodimers. Journal of Physical Chemistry C, 2012, 116, 10390-10395.	1.5	31
182	Template-free synthesis of large anisotropic gold nanostructures on reduced graphene oxide. Nanoscale, 2012, 4, 3055.	2.8	28
183	Modeling of drug release from biodegradable tripleâ€ ł ayered microparticles. Journal of Biomedical Materials Research - Part A, 2012, 100A, 3353-3362.	2.1	9
184	Synthesis and Structure Characterization of a Stable Nonatwistacene. Angewandte Chemie - International Edition, 2012, 51, 6094-6098.	7.2	199
185	Correlated Optical Measurements and Plasmon Mapping of Silver Nanorods. Nano Letters, 2011, 11, 3482-3488.	4.5	125
186	Patterning of Plasmonic Nanoparticles into Multiplexed One-Dimensional Arrays Based on Spatially Modulated Electrostatic Potential. ACS Nano, 2011, 5, 8288-8294.	7.3	62
187	Synthesis of hexagonal close-packed gold nanostructures. Nature Communications, 2011, 2, 292.	5.8	553
188	Controlled Synthesis of Ag/Ag/C Hybrid Nanostructures and their Surfaceâ€Enhanced Raman Scattering Properties. Chemistry - A European Journal, 2011, 17, 13386-13390.	1.7	9
189	Periodic Electric Field Enhancement Along Gold Rods with Nanogaps. Angewandte Chemie - International Edition, 2010, 49, 78-82.	7.2	41
190	A systems approach towards the stoichiometry-controlled hetero-assembly of nanoparticles. Nature Communications, 2010, 1, 87.	5.8	152
191	Gap Structure Effects on Surface-Enhanced Raman Scattering Intensities for Gold Gapped Rods. Nano Letters, 2010, 10, 1722-1727.	4.5	103
192	Silver-Based Nanodisk Codes. ACS Nano, 2010, 4, 5446-5452.	7.3	49
193	Free-Standing Bimetallic Nanorings and Nanoring Arrays Made by On-Wire Lithography. ACS Nano, 2010, 4, 7676-7682.	7.3	55
194	Electron-beam mapping of plasmon resonances in electromagnetically interacting gold nanorods. Physical Review B, 2009, 80, .	1.1	78
195	Chemical Fabrication of Heterometallic Nanogaps for Molecular Transport Junctions. Nano Letters, 2009, 9, 3974-3979.	4.5	105
196	Surprisingly Longâ€Range Surfaceâ€Enhanced Raman Scattering (SERS) on Au–Ni Multisegmented Nanowires. Angewandte Chemie - International Edition, 2009, 48, 4210-4212.	7.2	90
197	Plasmonâ€Mediated Synthesis of Silver Triangular Bipyramids. Angewandte Chemie - International Edition, 2009, 48, 7787-7791.	7.2	151
198	Confining Standing Waves in Optical Corrals. ACS Nano, 2009, 3, 615-620.	7.3	66

Sниzнои Li

#	Article	IF	CITATIONS
199	Plasmonic Focusing in Rodâ^'Sheath Heteronanostructures. ACS Nano, 2009, 3, 87-92.	7.3	51
200	Coreâ^'Shell Triangular Bifrustums. Nano Letters, 2009, 9, 3038-3041.	4.5	84
201	Methods for Describing the Electromagnetic Properties of Silver and Gold Nanoparticles. Accounts of Chemical Research, 2008, 41, 1710-1720.	7.6	457
202	Electrochemical Approach to and the Physical Consequences of Preparing Nanostructures from Gold Nanorods with Smooth Ends. Journal of Physical Chemistry C, 2008, 112, 15729-15734.	1.5	28
203	From Discrete Electronic States to Plasmons: TDDFT Optical Absorption Properties of Ag _{<i>n</i>} (<i>n</i> = 10, 20, 35, 56, 84, 120) Tetrahedral Clusters. Journal of Physical Chemistry C, 2008, 112, 11272-11279.	1.5	252
204	Surface Plasmon-Mediated Energy Transfer in Heterogap Auâ^'Ag Nanowires. Nano Letters, 2008, 8, 3446-3449.	4.5	59
205	The Effect of Surface Roughness on the Extinction Spectra and Electromagnetic Fields around Gold Nanoparticles. Materials Research Society Symposia Proceedings, 2008, 1087, 10801.	0.1	4
206	Vibrational Spectral Diffusion of Azide in Waterâ€. Journal of Physical Chemistry B, 2006, 110, 18933-18938.	1.2	66
207	Vibrational energy relaxation of azide in water. Journal of Chemical Physics, 2006, 125, 244507.	1.2	36
208	Approaches for the calculation of vibrational frequencies in liquids: Comparison to benchmarks for azide/water clusters. Journal of Chemical Physics, 2006, 124, 204110.	1.2	66
209	Mechanism of Chromyl Chloride Epoxidation. Journal of the American Chemical Society, 2003, 125, 11188-11189.	6.6	11
210	Generation of laserâ€driven flyer dominated by shockâ€induced shear bands: A molecular dynamics simulation study. Chinese Physics B, O, , .	0.7	0